Performance of a *q*-plate tunable retarder in reflection for the switchable generation of both first and second order vector beams

María M. Sánchez-López,[1,*] Jeffrey A. Davis,[2] Nobuyuki Hashimoto,[3] Ignacio Moreno,[4] Enrique Hurtado,[2] Katherine Badham,[2] Ayano Tanabe,[3] and Sam W. Delaney[2]

[1]*Instituto de Bioingeniería, Universidad Miguel Hernández, 03202 Elche, Spain*
[2]*Department of Physics, San Diego State University, San Diego, CA 92182-1233, USA*
[3]*Development Division, Citizen Holdings Co., Ltd, Saitama, 359-8511, Japan*
[4]*Departamento de Ciencia de Materiales, Óptica y Tecnología Electrónica. Universidad Miguel Hernández, 03202 Elche, Spain*
**Corresponding author: mar.sanchez@umh.es*

Received XX Month XXXX; revised XX Month, XXXX; accepted XX Month XXXX; posted XX Month XXXX (Doc. ID XXXXX); published XX Month XXXX

We examine the performance of a tunable liquid crystal *q*-plate in a reflective geometry. When the device is tuned to a half-wave retardance, it operates as a *q*-plate with twice the value (2*q*) by adding a quarter-wave retarder between the mirror and the *q*-plate. However, when the device is tuned to a quarter-wave retardance, it acts as the original *q*-plate without the retarder. Experimental results are shown. Using an input tunable polarization state generator, the system allows the switchable production of all states on both the first and second order Poincaré spheres. © 2015 Optical Society of America

OCIS codes: *(230.3720) Liquid-crystal devices; (230.5440) Polarization-selective devices; (120.5410) Polarimetry.*

http://dx.doi.org/10.1364/OL.41.000013

Optical retarder elements with azimuthal rotation of the principal axes are receiving a great deal of attention due to their ability to create cylindrically polarized vector beams, and to transfer orbital angular momentum (OAM) to light [1]. Both OAM and vector beam multiplexing are being investigated as promising new techniques for optical communications [2-3]. Therefore, devices capable of switching between different beam configurations are of interest, especially if they can be tuned at high speed [4]. This is the case of the *q*-plates [5,6], which are half-wave retarders where the principal axis rotates with the azimuth angle. These *q*-plates are defined by the degree to which the principal axis rotates with the azimuthal angle. For $q=1/2$, the principal axis rotates through π radians, while it rotates through 2π radians for $q=1$ as shown in Fig. 1. These devices can be fabricated with special liquid crystal patterns [7-9], or by a local polarization transformation of metasurfaces [6,10]. The retardance of liquid crystal *q*-plates can be tuned electronically.

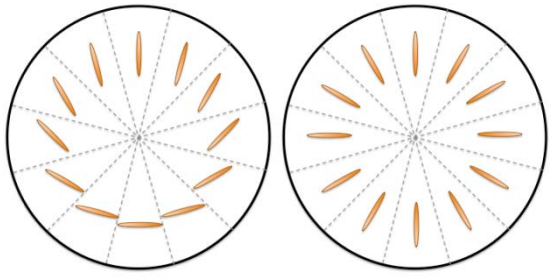

Fig. 1. Axis structure of *q*-plates with (a) $q=1/2$, (b) $q=1$.

However the orientation of the liquid crystal director axes remains fixed, with the *q*-value defined in the fabrication design.

These devices produce higher order cylindrically polarized vector fields with a polarization state that varies spatially with axial symmetry [11]. Such cylindrically polarized vector beams can be represented in the higher order Poincaré spheres [10,12-14], which are generalizations of the standard sphere employed to describe a beam of light with uniform polarization. The control of the input polarization can be used to generate different paths in the generalized Poincaré sphere, as has been demonstrated using systems with rotatable half-wave (HWP) and quarter-wave (QWP) plates [15]. However different devices are required to address the Poincaré spheres of different orders.

The idea of using a *q*-plate in a geometry that allows two passes through the device was used in [16] to switch between OAM values ±2 and ±4 by rotating two QWPs. By contrast, in this Letter, we introduce a reflective geometry that allows a given *q*-plate to be switched between the standard operation, with the designed *q* value, to the doubled value 2*q*. The system requires that the retardance of the *q*-plate be tuned at $\pi/2$ or at π radians, and it must be combined with another uniform linear retarder, with zero and quarter-wave

retardance respectively. In comparison with the proposal in [16], our system is acting as an equivalent higher order q-plate and therefore cannot only change the OAM content of the input beam, but also can generate all vector beams in either the first or second order Poincaré spheres with the same device.

The general q-plate Jones matrix can be expressed as that of a phase-plate retarder with retardance ϕ where the principal axis follows q times the azimuthal angle θ as:

$$\mathbf{M}_q(\phi) = \mathbf{R}(-q\theta)\cdot \mathbf{W}(\phi)\cdot \mathbf{R}(+q\theta), \qquad (1)$$

where $\mathbf{R}(\theta)$ and $\mathbf{W}(\phi)$ are the rotation and aligned linear retarder matrices as:

$$\mathbf{R}(\theta)=\begin{pmatrix} \cos(\theta) & \sin(\theta) \\ -\sin(\theta) & \cos(\theta) \end{pmatrix}, \quad \mathbf{W}(\phi)=\begin{pmatrix} e^{+i\phi/2} & 0 \\ 0 & e^{-i\phi/2} \end{pmatrix}, \qquad (2)$$

The q-plate presents an efficiency conversion from circular RCP to LCP (or reversed) given by $\sin^2(\phi/2)$ [17] and reaches 100% efficiency when it is tuned to a half-wave retardance, $\phi = m\pi$ (m=1,3,5,...). In this situation, the Jones matrix in Eq. (1) is given by [3]:

$$\mathbf{M}_q(\phi=\pi)=\begin{pmatrix} \cos(2q\theta) & \sin(2q\theta) \\ \sin(2q\theta) & -\cos(2q\theta) \end{pmatrix}. \qquad (3)$$

Our experimental q-plate is a prototype from Citizen Holdings Co. [18] with 12 liquid crystal segments with a diameter of 2.5 cm, where q=1/2, as shown in Fig. 1(a). The phase of each segment can be varied using an applied voltage. The segmented structure of the device gives an excellent polarization conversion efficiency of 97.7% [18].

First, we characterized the q-plate retardance in a standard transmission setup for the 633 nm wavelength. The input left circular polarization (LCP) was generated using high quality linear polarizers and QWPs (Meadowlark Optics DPM-200-VIS and NQM-200-0633 respectively). The right circular polarization (RCP) state was detected using an equivalent system and a Newport Corp. model 920 detector. The retardance was adjusted by changing the voltage of a 1 kHz square wave. The results in Fig. 2, follow the expected $\sin^2(\phi/2)$ behavior, with the retardance decreasing towards zero as the voltage increased over a tuning range of 5π radians [18]. The H, Q, and F points correspond to half-wave, quarter-wave and full-wave retardances respectively.

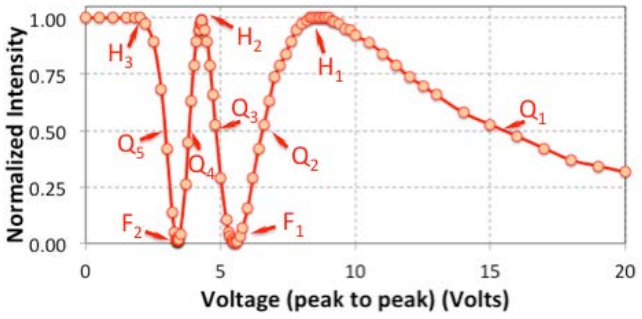

Fig. 2. Normalized intensity for the LCP to RCP calibration of the q-plate retardance in transmission for wavelength λ=633 nm.

Next we study the operation of the q-plate in a reflective geometry as shown in Fig. 3. The vertically polarized input beam enters a non-polarizing beam-splitter (NPBS). The transmitted beam passes through the q-plate and a vertically aligned linear retarder (LR) with retardance δ. The beam reflects from a mirror and passes back through the LR and the q-plate. Although this geometry suffers 75% intensity loss due to the use of the NPBS, it allows the generation of vector beams that cannot be generated with polarizing beam splitters.

This geometry can be analyzed following the theory in [19,20]. The reflection at the mirror is described by the matrix $\mathrm{J}=\mathrm{diag}(1,-1)$. Note that this yields the same effect as the vertically aligned HWP in Eq. (2), since $\mathrm{W}(\pi)=i\,\mathrm{J}$. We define $\mathbf{M}$ as the Jones matrix of a reciprocal anisotropic polarization element between the NPBS and the mirror (in our case the q-plate and the LR). Then, the Jones matrix for the same element in the opposite direction is given by $\mathbf{J}\mathbf{M}^t\mathbf{J}$, where t stands for the transposed matrix. Finally, another reflection occurs at the NPBS that is described by another $\mathbf{J}$ matrix. However, the NPBS may introduce some retardance. We compensated this with a Soleil-Babinet compensator placed at the output of the NPBS, whose retardance was adjusted to eliminate the additional retardance.

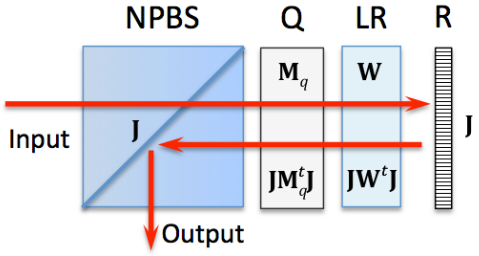

Fig. 3. Optical system: NPBS: non-polarizing beam splitter; Q: q-plate; LR: linear retarder; R: mirror reflector.

Therefore the system in Fig. 3 can be written and simplified as the following Jones matrix sequence [19,20]:

$$\mathbf{M}_{ref} = \mathbf{J}\cdot\left[\mathbf{J}\mathbf{M}_q^t\mathbf{J}\right]\cdot\left[\mathbf{J}\mathbf{W}^t\mathbf{J}\right]\cdot\mathbf{J}\cdot\mathbf{W}\cdot\mathbf{M}_q = \mathbf{M}_q^t\cdot\mathbf{W}^t\cdot\mathbf{W}\cdot\mathbf{M}_q, \qquad (4)$$

where we used $\mathbf{J}\cdot\mathbf{J}=\mathbf{I}$, where $\mathbf{I}$ is the identity matrix. Applying Eqs. (1) and (2), the Jones matrix of the reflection system in Fig. 3 can be written as

$$\mathbf{M}_{ref} = \mathbf{R}(-q\theta)\mathbf{W}(\phi)\mathbf{R}(+q\theta)\cdot\mathbf{W}(2\delta)\cdot\mathbf{R}(-q\theta)\mathbf{W}(\phi)\mathbf{R}(+q\theta). \qquad (5)$$

where we used the relations $(\mathbf{AB})^t=\mathbf{B}^t\mathbf{A}^t$ and $\mathbf{W}^t=\mathbf{W}$.

Now we examine two specific cases. In the first case the q-plate is tuned to a quarter-wave retardance $\phi=\pi/2$, while the LR is set to δ=0. Therefore, the matrix in Eq. (5) is now:

$$\mathbf{M}_{ref} = \mathbf{R}(-q\theta)\mathbf{W}(\pi)\mathbf{R}(+q\theta). \qquad (6)$$

Here we used the relations $\mathbf{R}(+q\theta)\mathbf{R}(-q\theta)=\mathbf{I}$ and $\mathbf{W}(\pi/2)\mathbf{W}(\pi/2)=\mathbf{W}(\pi)$. Equation (6) shows that the double pass through the q-plate tuned at retardance $\pi/2$ doubles its effective retardance, and makes it operate in reflection as the standard q-plate with π retardance.

To verify this case, we used our q=1/2 plate to generate the first-order polarized beams by illuminating the reflection system in Fig. 3 with uniformly polarized light beams. The input polarization is controlled through the polarization state generator (PSG) in Fig. 4 [18]. It consists of a vertically oriented linear polarizer (LP), a linear retarder (LR1) oriented at 45^0, and a polarization rotator composed of a second vertically oriented linear retarder (LR2) between two QWPs at $\pm 45^0$. This system generates any state of polarization by tuning the retardances ϕ_1 and ϕ_2.

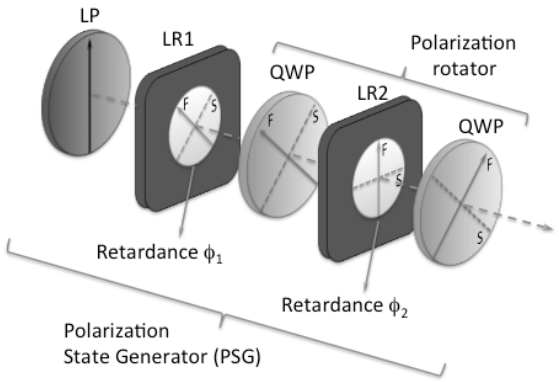

Fig. 4. Polarization state generator (PSG) system to produce arbitrary state of polarization through tuning of retardances ϕ_1 and ϕ_2.

Therefore, this PSG can be controlled fully electronically by means of electro-optic retarders. As stated previously, there is great interest in using *q*-plates in high-speed optical fiber multiplexing systems. This system in Fig. 4 does not involve any physical rotation of the optical elements and, therefore, is capable to achieve GHz speeds if fast electro-optic modulators are employed as variable retarders.

Experimental results for the production of the first order vector beams are presented in Fig. 5. We generated the six cardinal points of the first order Poincaré sphere, namely, radial, azimuthal, two slanted and the two circular LCP and RCP polarized beams. They are obtained by adjusting the retardances ϕ_1 and ϕ_2 at the PSG system in Fig. 4, to generate input linear states at 0^0, 45^0, 90^0 and 135^0, and RCP and LCP states. These beams are the input to the reflection system in Fig 3. Each row in Fig. 5 shows the beam emerging from the system, without an analyzer, and after passing through a linear analyzer oriented at zero, 45^0, 90^0 and 135^0, and LCP and RCP circular polarizers. The intensity patterns agree with the expected polarization distribution. The zero intensity in the center of the beam indicates the generation of the axial vortex. Note the extremely dark images when LCP (or RCP) is incident and RCP (or LCP) is detected. Since we are using high-quality linear polarizers and wave plates, the contrast ratio of the system is very high.

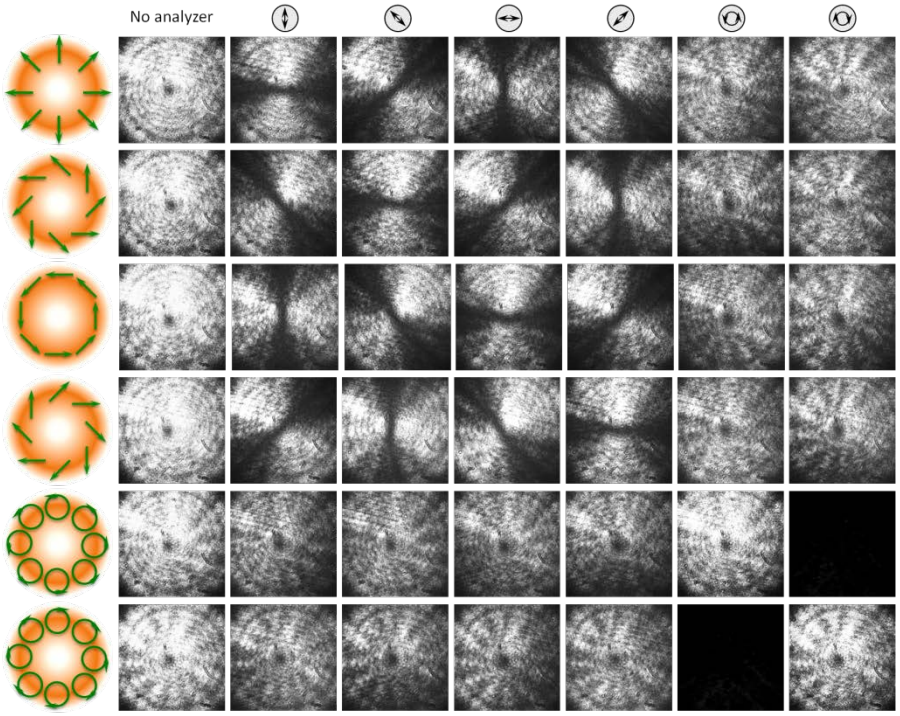

Fig. 5. Generation of vector beams in the first-order Poincaré sphere. An equivalent *q*-plate with $q=1/2$ is obtained by tuning the LR to zero retardance and the *q*-plate to a quarter-wave retardance. The polarization analyzer applied in each case is indicated on the top of the figure.

In the second case, the *q*-plate is now tuned to a half-wave retardance $\phi=\pi$, while the linear retarder is set to a quarter-wave retardance $\delta=\pi/2$. The reflection system is given by

$$\mathbf{M}_{ref} = \mathbf{R}(-q\theta)\mathbf{W}(\pi)\mathbf{R}(+q\theta)\cdot\mathbf{W}(\pi)\cdot\mathbf{R}(-q\theta)\mathbf{W}(\pi)\mathbf{R}(+q\theta) = \\ = -i\mathbf{R}(-2q\theta)\mathbf{W}(\pi)\mathbf{R}(+2q\theta) \qquad (7)$$

where we used the relations $\mathbf{W}(\pi) = i\mathbf{J}$ and $\mathbf{R}(+\theta)\mathbf{J} = \mathbf{J}\mathbf{R}(-\theta)$. Now, the comparison of Eq. (7) and Eq. (1) reveals that this second case results again in a π retardance *q*-plate but, interestingly, its *q* value is twice that of the first case.

Figure 6 shows the experimental results for this second case ($\phi=\pi$, $\delta=\pi/2$). Now, the $q=1$ plate behavior is verified by the generation of the second order vector beams. Again, the six cardinal points, now of the second order Poincaré sphere, are obtained by illuminating the system with the same six input states as before, generated in the PSG in Fig. 4. The intensity patterns agree with the second-order expected polarization distributions. Note, for instance, the four dark angular directions when the system is illuminated with linearly polarized light and analyzed with a linear polarizer. In addition, the axial zero intensity now appears with a larger diameter, confirming the doubled topological charge.

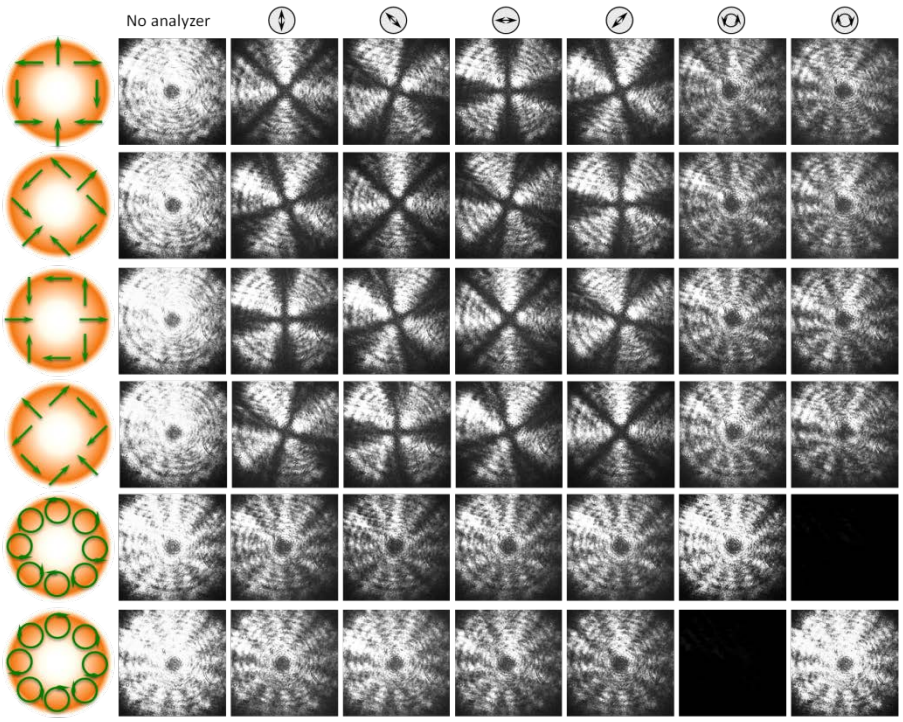

Fig. 6. Generation of vector beams in the second order Poincaré sphere. An equivalent q-plate with q=1 is obtained by tuning the LR to quarter-wave retardance and the q-plate to a half-wave retardance. The polarization analyzer applied in each case is indicated on the top.

In conclusion, we have developed a reflection system that allows the electronic switching between a given q-plate and a doubled q valued device. The system can be applied to q-plates with tunable retardance, and it requires a tunable LR placed between the q-plate and the mirror. When the q-plate is tuned to a $\pi/2$ retardance and the LR to a zero retardance, the system acts as the original q-plate. However when the q-plate is tuned to a π retardance and the LR acts as a quarter-wave retarder, the system acts as a q-plate with a doubled q charge. Experimental results are shown using a prototype q-plate device developed by Citizen Holdings Co., Ltd.

These results are important for several reasons. The q-value in q-plate devices is fixed at the fabrication step. Our technique allows to switch a q-plate between two values, and could be applied for the high speed generation of first- and second-order vector beams in combination with the PSG system in Fig. 4 if fast electro-optic modulators are employed.

Funding. Ministerio de Ciencia e Innovación (MICINN) (FIS2012-39158-C02-02).

References

1. A. M. Yao, and M. J. Padget, Adv. Opt. Photon. **3**, 161–204 (2011).
2. J. Wang, J.-Y. Yang, I.M. Fazal, N. Ahmed, Y. Yan, H. Huang, Y. Ren, Y. Yue, S. Dolinar, M. Tur, and A.E. Willner, Nat. Photonics **138**, 488-496 (2012).
3. G. Milione, M. P. J. Lavery, H. Huang, Y. Ren, G. Xie, T. A. Nguyen, E. Karimi, L. Marrucci, D. A. Nolan, R. R. Alfano, and A. E. Willner, Opt. Lett. **40**, 1980-1983 (2015).
4. P. Gregg, M. Mirhosseini, A. Rubano, L. Marrucci, E. Karimi, R.W. Boyd, and S. Ramachandran, Opt. Lett. **40**, 1729-1732 (2015).
5. L. Marrucci, C. Manzo, and D. Paparo, Phys. Rev. Lett. **96**, 163905 (2006).
6. M. Beresna, M. Gecevičius, P. G. Kazansky, and T. Gertus, Appl. Phys. Lett. **98**, 201101 (2011).
7. M. Stalder and M. Schadt, Opt. Lett. **21**, 1948-1950 (1996).
8. S. Slussarenko, A. Murauski, T. Du, V. Chigrinov, L. Marrucci, and E. Santamato, Opt. Express **19**, 4085-4090 (2011).
9. S. Slussarenko, B. Piccirillo, V. Chigrinov, L. Marrucci, and E. Santamato, J. Opt. **15**, 025406 (2013).
10. Y. Liu, X. Ling, X. Yi, X. Zhou, H. Luo, and S. Wen, Appl. Phys. Lett. **104**, 191110 (2014).
11. Q. Zhan, Adv. Opt. Photon. **1**, 1–57 (2009).
12. A. Holleczek, A. Aiello, C. Gabriel, C. Marquardt, and G. Leuchs, Opt. Express **19**, 9714-9736 (2011).
13. G. Milione, H. I. Sztul, D. A. Nolan, and R. R. Alfano, Phys. Rev. Lett. **107**, 053601 (2011).
14. S. Chen, X. Zhou, Y. Liu, X. Ling, H. Luo, and S. Wen, Opt. Lett. **39**, 5274-5276 (2014).
15. F. Cardano, E. Karimi, S. Slussarenko, L. Marrucci, C. de Lisio, and E. Santamato, Appl. Opt. **51**, C1-C8 (2012).
16. S. Slussarenko, E. Karimi, B. Piccirillo, L. Marrucci, and E. Santamato, J. Opt. Soc. Am. A **28**, 61-65 (2011).
17. B. Piccirillo, V. D'Ambrosio, S. Slussarenko, L. Marrucci, and E. Santamato, Appl. Phys. Lett. **97**, 241104 (2010).
18. J. A. Davis, N. Hashimoto, M. Kurihara, E. Hurtado, M. Pierce, M. M. Sánchez-López, K. Badham, and I. Moreno, Appl. Opt. **54**, 9583-9590 (2015).
19. C. R. Fernández-Pousa, I. Moreno, N. Bennis, and C. Gómez-Reino, J. Soc. Opt. Am. A **17**, 2074-2080 (2000).
20. I. Moreno, C. R. Fernández-Pousa, J. A. Davis, and D. J. Franich, Opt. Eng. **40**, 2220-2226 (2001).